Anthropogenic VOCs in the Long Island Sound, NY Airshed and their Role in Ozone Production

Allison M. Ring[1], Russell R. Dickerson[1], Abby E. Sebol[1], Xinrong Ren[2], Sarah E. Benish[1,*], Ross J. Salawitch[1,3,4], Andrea Galasyn[5], Paul J. Miller[6] and Timothy P. Canty[1]

[1] Department of Atmospheric and Oceanic Science, University of Maryland, College Park, MD

[2] Atmospheric Sciences Modeling Division, NOAA Air Resources Laboratory, College Park, MD

[3] Department of Chemistry and Biochemistry, University of Maryland, College Park, MD

[4] Earth System Science Interdisciplinary Center, University of Maryland, College Park, MD

[5] Maine Department of Environmental Protection, Bureau of Air Quality, Augusta, ME

[6] Northeast States for Coordinated Air Use Management, Boston, MA

[*] Now at: Office of Air Quality Planning & Standards, US Environmental Protection Agency, Durham, NC

Corresponding author: Allison M. Ring (aring1@umd.edu)

20 **Abstract**

21   Cities like New York and areas downwind have poor air quality due to pollution

22 generated by human activity. Ozone (O_3), a harmful pollutant, is produced in the atmosphere

23 from photochemical reactions involving volatile organic compounds (VOCs) and nitrogen oxides

24 (NO_x). Aircraft measurements of VOCs obtained during an O_3 event in May 2017 over the New

25 York City metropolitan area, Long Island Sound, and Connecticut show concentrations of O_3

26 exceeding 100 ppb between ~200 – 500 meters above the surface. During this campaign, 35

27 whole air canisters were collected, and 50 VOC species were measured. Biogenic isoprene often

28 dominates VOC reactivity in summer months, but analysis of the chemistry in the middle of the

29 Planetary Boundary Layer (PBL) indicates that primary anthropogenic VOCs such as propylene

30 and isopentane played a major, possibly dominant role in this Spring 2017 O_3 event and are

31 suitable targets for control.

32   The most important measured anthropogenic VOCs ranked by OH reactivity were

33 propylene and isopentane, with n-butane and 1-pentene also playing a substantial role. The most

34 important anthropogenic VOCs ranked by Ozone Formation Potential (OFP) were again

35 propylene and isopentane, but aromatic species like toluene were also large contributors.

36 Isoprene ranked tenth in importance for OFP. For VOC species with short lifetimes, like isoprene

37 and propylene, mixing of air parcels throughout the PBL means air above the surface may

38 quickly become depleted of these VOCs, allowing longer-lived, anthropogenic VOCs to have a

39 proportionally greater impact on photochemical O_3 production aloft. Our observations indicate

40 that VOC reactivity was much larger in the morning than in the afternoon, suggesting controls of

41 propylene, isopentane, and aromatics overnight may be useful for reducing morning

42 concentrations of VOCs and therefore possibly reduce maximum concentrations of O_3 observed

43 in the afternoon. Finally, because formaldehyde (HCHO) was not measured during these flights,

44 and since oxygenates also contribute to O_3 formation, we estimate the relative contribution of

45 isoprene and propylene to HCHO formation using a box model. Propylene produces ~25% and

46 isoprene produces ~4% of HCHO within the box model.

47 **Keywords:**

48   Air Quality, Long Island Sound Tropospheric Ozone Study (LISTOS), Ozone production

49 regime, Anthropogenic VOCs, Maximum Incremental Reactivity, Ozone Formation Potential

50 **1: Introduction**

51   The National Ambient Air Quality Standards (NAAQS), established by the United States

52 Environmental Protection Agency (EPA) under the federal Clean Air Act, set national levels for

53 six criteria pollutants deemed harmful to human health and welfare [*EPA*, 1970; 1990]. EPA

54 reconsiders the NAAQS periodically and has increased the stringency of the surface ozone (O_3)

55 standard over time, with the most recent revision occurring in 2015. As of October 2022, the

56 New York City (NYC) metropolitan area is in non-attainment of both the older 2008 and more

57 recent 2015 O_3 NAAQS, which are 75 parts per billion (ppb) and 70 ppb for an 8 hour average,

58 respectively [*EPA*, 2016a; *Federal_Register*, 2022a; b]. Areas with particularly poor air quality,

59 such as the NYC region, must use EPA-approved air quality models to develop strategies

60 demonstrating how they will reach attainment. Observational studies can support these modeling

61 efforts by identifying the meteorological and chemical conditions, emission sources, and the

62 specific atmospheric species most important for the photochemical production of tropospheric

63 O_3.

64   Located downwind from NYC, Connecticut (CT) frequently receives on-shore

65 atmospheric circulation of anthropogenic emissions exported from NYC over Long Island Sound

66 (LIS) [*Caicedo et al.*, 2021; *Han et al.*, 2022; *Torres-Vazquez et al.*, 2022; *Wu et al.*, 2021],

67 similar to bay-breezes advecting polluted air from the Chesapeake Bay over the Baltimore, MD

68 region [*Loughner et al.*, 2014; *Mazzuca et al.*, 2017; *Stauffer et al.*, 2015]. All of CT, including

69 its coastline, is presently designated as in non-attainment of the 2015 O_3 standard

70 [*Federal_Register*, 2022a]. CT, along with New Jersey and New York, will need to perform air

71 quality modeling that identifies the upwind sources, including those from states outside the NYC

72 metropolitan area, that contribute to poor air quality throughout the region.

73   Identifying volatile organic compounds (VOCs) most important for photochemical O_3

74 production is an area of active research. Previous studies have identified many biogenic and

75 anthropogenic VOCs that impact air quality, especially during summer months [*Baker et al.*,

76 2008; *Kleinman*, 2000]. *McDonald et al.* [2018] showed with a review of U.S. emissions

77 inventories and box modeling analyses that VOCs from pesticides, adhesives, personal care

78 products, cleaning agents, etc. (collectively called Volatile Chemical Products (VCPs)) are

79 important sources of urban VOCs. They showed that VCPs significantly impact ground-level

80 outdoor and indoor air quality in Pasadena, California and throughout the Los Angeles basin. In

81 the Long Island Sound Tropospheric Ozone Study (LISTOS) study region, *Coggon et al.* [2021]

82 showed that VCPs, especially anthropogenically produced monoterpenes, add significantly to the

83 total VOC burden in the NYC metropolitan region. Inclusion of chemistry associated with

84 oxygenated VCPs contributed to the production of peroxyacetyl nitrate (PAN), critical for the

85 model to achieve the high O_3 concentrations observed in the NYC metropolitan region during the

86 summer of 2018. Both *McDonald et al.* [2018] and *Coggon et al.* [2021] show the importance of

87 other anthropogenic VOCs in addition to those from biogenic and fossil fuel sources, especially

88 in densely populated metropolitan regions. Inclusion of VCPs along with mobile and

89 petrochemical VOC sources in model emissions inventories will be necessary to bring modeled

90   and observed OH reactivity and secondary organic aerosol formation in urban centers into

91   agreement [*Seltzer et al.*, 2021]. Monoterpenes along with sesquiterpenes and diterpenes also

92   have biogenic sources. These emissions occur throughout the day and evening, contributing to a

93   buildup of terpene concentrations at night [*Li et al.*, 2020]. High evening concentrations of

94   terpenes likely lead to O_3 scavenging and further contribute to the reduced concentrations of O_3

95   at night. Examination of terpenes in addition to isoprene is beyond the scope of this paper as

96   these VOCs were not measured during these aircraft flights, but more field missions and ground-

97   based monitoring of these VOCs are necessary because they are important components to

98   understanding atmospheric O_3 formation. Various research groups are working to improve

99   terpene chemistry in air quality models [*Schwantes et al.*, 2020], and observations of these

100   species will be useful for validation.

101   *Chen et al.* [2019] conducted a thorough analysis comparing VOCs measured in aircraft

102   campaigns over North America to model simulations. They found isoprene generally dominates

103   VOC reactivity across the US but recognized this result may not be true for polluted urban

104   regions. They explicitly excluded from their analysis observations of highly polluted air masses

105   (NO_2 > 4 ppbv) and recent biomass burning (CH_3CN > 0.2 ppbv) and called for more research to

106   understand the complex VOC chemistry in urban centers. Our study complements *McDonald et*

107   *al.* [2018], *Coggon et al.* [2021], and *Chen et al.* [2019] by examining airborne observations of a

108   suite of anthropogenic VOCs in the polluted NYC Metropolitan region that play an important

109   role in O_3 formation near this urban center and areas downwind. While it is clear from

110   *McDonald et al.* [2018] and *Coggon et al.* [2021] that VCPs and oxygenates are quite important

111   to air quality, measurements of these VOCs are not yet widely available due to methodology

112   limitations. This study focuses on primary VOCs with a long history of monitoring, well-

113   established methods of analysis, and VOCs that are inventoried, regulated and controllable. Our

114   flight campaign provides observations throughout the Planetary Boundary Layer (PBL) of O_3 as

115   well as these primary VOCs, typically observed only from the surface at monitoring locations

116   like the Photochemical Assessment Monitoring Stations (PAMS) sites, which *Hembeck et al.*

117   [2019] showed may be missing important VOCs.

118

119   **2: Methods and Data**

120   *Carter* [1994] detailed the development of a metric known as the Maximum Incremental

121   Reactivity (MIR) to represent the relative importance of individual VOCs to surface O_3

122   production. The MIR scale is derived from smog chamber analysis and photochemical box-

123   modeling of VOC-sensitive O_3 production scenarios, meaning VOCs have the maximum impact

124   on O_3 production. To calculate MIR, *Carter* [1994] performed two model simulations: a baseline

125   VOC-sensitive simulation, and one with VOCs added to the emissions that produced a linear

126   increase in O_3. The difference in the amount of O_3 produced between the two simulations,

127   divided by the amount of VOC added, yields the MIR (g O_3 produced / g of VOC added)

128   [*Carter*, 1994]. A significant refinement of previously calculated MIR values for VOCs was

129   performed by *Carter* [2010], and further improvements to MIR values using representative urban

130   atmospheres were conducted by *Venecek et al.* [2018]. All subsequent analysis in this study is

131   conducted using the updated MIR values from *Venecek et al.* [2018].

132   To identify the anthropogenic VOCs that may have been major contributors to the high

133   O_3 event in Spring 2017, we calculate the Ozone Formation Potential (OFP) of each VOC. Here,

134   OFP represents the amount of O_3 (ppbv) that could potentially be formed under ideal

135   atmospheric circumstances based on the amount of VOC present and its associated MIR value

136 (equation 1) [*Tang et al.*, 2007]. The MIR calculation is based on varying VOC emissions and

137 determining the resulting increase in O_3, so this quantity is best applied to VOC emissions. The

138 formula for OFP is:

139 $$OFP = MIR \times [VOC] \tag{1}$$

140   In this work, MIR is used to calculate OFP based on observed VOC concentrations.

141 Therefore, OFP found in this manner is a lower limit to the potential O_3 formed in the actual

142 atmosphere, especially for the VOCs with short lifetimes such as alkenes since much of the

143 original emission has already reacted in the atmosphere before it can be measured. For those

144 VOCs with longer lifetimes, this method may be a better approximation of the actual OFP. This

145 metric we use places MIR into quantifiable terms, allowing air quality planners to establish

146 bounds for the potential production of O_3 based on each VOC and identify target species and

147 emission sources to control. Unlike OH reactivity, OFP accounts for compounds and radicals

148 produced in subsequent oxidation steps.

149   We analyze data collected from three research flights conducted over LIS and CT in May

150 2017 that provide *in situ* measurements of VOCs and other atmospheric species during an O_3

151 exceedance event. The reactivity with OH and the OFP for each VOC are calculated and ranked

152 in order of importance, providing air quality policy makers with a list of VOCs most critical to

153 the production of O_3 in the LIS region during this exceedance event.

154 **2.1: Aircraft Data**

155   For the past two decades, the University of Maryland has led a multi-faceted effort to

156 understand air quality in the Eastern U.S. called the Regional Atmospheric Measurement

157 Modeling and Prediction Program (RAMMPP) (http://www.atmos.umd.edu/~rammpp). *In situ*

158 aircraft measurements are collected during the O_3 season (April – October) providing

159   information about long-term trends in the Mid-Atlantic and Eastern U.S. [*He et al.*, 2013;

160   *Taubman et al.*, 2004]. For this study, a small portion of the RAMMPP data are used to analyze

161   VOCs in the LIS region of New York on May 17 and 18, 2017. These data were collected during

162   a high O_3 event, over the course of three research flights with the intent of sampling air within

163   the boundary layer, from near the surface to ~1500 m altitude.

164   Trace gas and aerosol measurements were collected by University of Maryland

165   researchers aboard a Cessna 402B aircraft. A complete description of the aircraft's

166   instrumentation setup can be found in *Ren et al.* [2018]. A total of 35 whole air canisters

167   (hereafter simply called cans) sampling ambient air mostly between 250 – 500 m above the

168   surface were collected, and 50 VOC species were reported for each can during this field

169   campaign. The list of species can be found in the supplemental information (Table S1). All can

170   samples were processed by the Maine Department of Environmental Protection (DEP) using

171   Standard Operating Procedures (SOP) [*MaineDEP*, 2017] in accordance with the National Air

172   Toxics Trends Station technical assistance document [*EPA*, 2016b]. Samples were analyzed

173   using a Gas Chromatograph (Agilent 7890A GC System) coupled to a Mass Spectrometer

174   (Agilent 5975C Inert MSD) and referenced to a NIST traceable certified TO-15 VOC standard.

175   Preceding any analysis, the GC/MS is tested to ensure attainment of the instrument performance

176   standard and is then calibrated within 24 hours prior to processing the can samples. The reported

177   VOC concentrations (ppbv) have an uncertainty of $\pm 20\%$ [*EPA*, 2016b; *MaineDEP*, 2017].

178   Two reference or blank cans were collected during the sample period. The average

179   reference can concentration for each VOC species was calculated and subtracted from the

180   corresponding measured VOC concentration in each sample can, correcting for any

181 contamination from the can interior or sample inlets. Maps of the three research flights and VOC

182 can collection locations are shown in Figure 1.
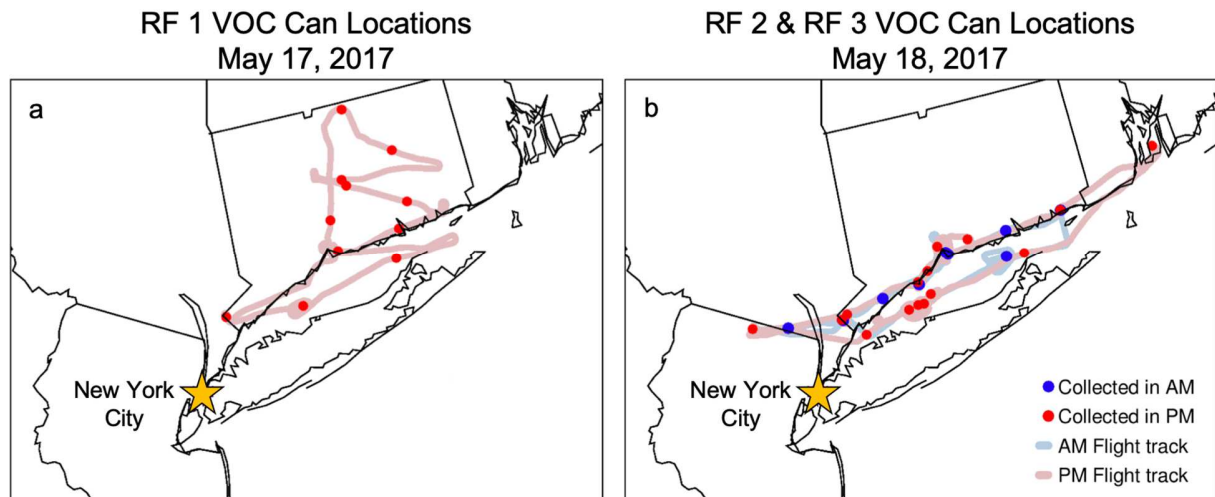
183

184 **Figure 1:** VOC can locations and research flight (RF) tracks over Connecticut and Long Island Sound (a) from
185 14:50 to 18:10 LST on May 17, 2017 and (b) from 7:40 to 10:25 LST (AM) and from 13:10 to 16:40 LST (PM) on
186 May 18, 2017. VOC cans were collected in flight and at various altitudes, with the vast majority within the boundary
187 layer. Color distinctions represent cans collected in the morning (blue) and in the afternoon (red). A total of 9 cans
188 were collected in the morning and a total of 26 cans were collected in the afternoon.

189

190   Figure 2 shows the archived Air Quality Index (AQI) maps for May 17 and 18, 2017

191 from the AirNow website. This forecasted O_3 exceedance event, early in the O_3 season,

192 motivated these research flights. Surface O_3 concentrations were forecast to reach unhealthy

193 levels for sensitive groups on May 17, escalating to unhealthy levels for everyone on May 18

194 along the CT coast north of the LIS [*AirNow*, Accessed 2018]. The measured surface 8-hour

195 average maximum O_3 and 1-hour maximum O_3 on May 17 and 18, 2017 for selected Air Quality

196 System (AQS) sites in NY and CT around LIS shown in Figure S1 are provided in Table S2. Of

197 the 18 total AQS sites examined, 9 sites were in exceedance of the NAAQS 2015 surface O_3

198 standard of 70 ppb on May 17, 2017, and 14 sites were in exceedance on May 18, 2017. The

199 maximum O_3 value measured along RF1 was 116 ppb, along RF2 was 81 ppb, and along RF3

200   was 130 ppb. Ambient temperatures peaked for the morning flight (RF2) at 82°F (27.8°C) and at

201   91°F (32.8°C) for both afternoon flights (RF1, RF3). Surface winds were westerly, generally

202   moving the NYC pollution plume over LIS and CT.
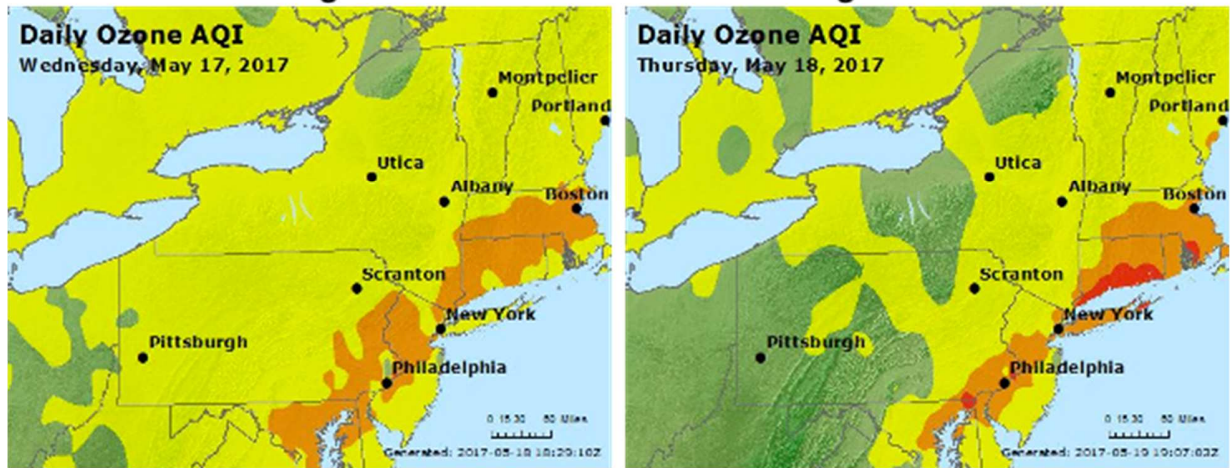
204   **Figure 2**: AirNow O_3 AQI forecast images for May 17 and 18, 2017. Yellow coloring indicates air quality is
205   acceptable however there may be a moderate health concern for people who are especially sensitive to pollution
206   (AQI: 51-100). Orange coloring indicates air quality is unsafe for sensitive groups like the elderly, children, and
207   people with respiratory problems (AQI: 101-150). Red coloring indicates air quality is unsafe and all people may
208   begin to experience health effects (AQI: 151-200). More information about AQI and the designations described
209   above can be found on the AirNow website https://www.airnow.gov. The images above can be found in the archives
210   located at http://files.airnowtech.org/?prefix=airnow/2017/.

211   Since 1998, approximately 14% of all O_3 exceedances in NJ, NY, and CT occur during

212   the meteorological spring (before June 1), and approximately 28% of exceedances occur during

213   the astronomical spring (before June 21). A table showing the spring exceedances, total number

214   of exceedances and percentage of spring exceedances for all three states for every year from

215   1998-2021 can be found in supplemental information (Table S3). A map of the monitoring sites

216   used to generate this table is shown in Figure S2. While there are fewer exceedances during the

217   spring than the summer months, exceedance events like the one in this study are not uncommon.

218   **3: Results and Discussion**

219   On May 17 and 18, 2017, the NYC metropolitan area suffered an O_3 event, with

220   Maximum Daily Average 8-hr O_3 (MDA8) reaching 84 ppb at the Stafford Hollow, CT site on

221   May 17 and 91 ppb at the Bridgeport, CT site on May 18, consistent with the forecasted Daily

222   Ozone AQI shown in Figure 2. Table S2 provides MDA8 and 1-hr Max values of O_3 at all AQS

223   sites in the LIS area. Figure 3 shows the observed O_3 and NO_x for all three RFs, binned every

224   500 meters. Both O_3 and NO_x were measured continuously along the flight tracks, providing

225   observations with high temporal resolution. As shown in Figure 3a high concentrations of O_3

226   were observed aloft, indicating photochemical O_3 production occurred throughout the PBL.

227   Further analysis shows elevated levels of SO_2 in conjunction with the high O_3 above 3000 meters

228   (Figure 3a), indicating a possible influence from powerplants via long-range transport. Figure S3

229   shows the vertical 500 meter binned profile of SO_2 and the temperature profile of the aircraft

230   spiral with the highest SO_2 measurement. A temperature inversion is evident at ~2500 meters

231   indicating the top of the PBL, providing further support for high SO_2 and O_3 transport in the

232   lower free troposphere. HYSPLIT ensemble back trajectories [*Stein et al.*, 2015] in Figure S4

233   provide further evidence for long-range transport of pollution by showing the air above the

234　temperature inversion with high SO_2 and O_3 originated over a region with numerous active

235　powerplants that emitted SO2 during these flights. HYSPLIT trajectories are initialized at the

236　height of the highest SO_2 measurement and are conducted for two days using archived 3 km

237　High Resolution Rapid Refresh meteorological input. The black dots in Figure S4 represent the

238　power plants in operation on May 16 and 17 according to Continuous Emissions Measurement

239　System (CEMS) data. To confirm the presence of synoptic meteorological conditions favorable

240　for atmospheric transport, we conducted two additional ensemble back trajectories initialized at

241　2500 meters and 3500 meters (Figure S4). A consistent pattern is discernable among all three

242　ensemble trajectories.

243　　　　The mixing time within the PBL is typically only a few hours on a warm sunny day,

244　meaning O_3 produced aloft or transported can mix down to the surface. Mixing of O_3, its

245　precursors and their intermediates throughout the PBL introduces uncertainty into determining

246　the O_3 production regimes in air parcels at the surface and higher in the PBL. Measurements of

247　species at the surface and aloft provide a more complete understanding of the local O_3

248　production regime, and therefore must be considered when trying to develop mitigation

249　strategies for O_3 exceedance events.

250

12
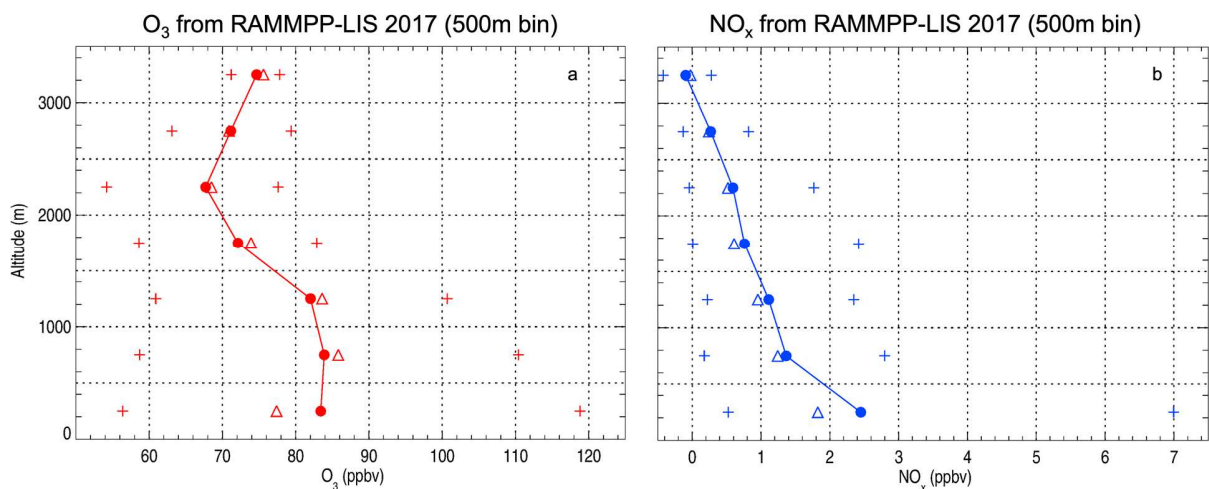
Figure 3: Observations of O_3 and NO_x from all flights over Long Island Sound conducted on May 17 (RF1) and May 18 (RF2, RF3) in 2017. (a) O_3 observations and (b) NO_x observations are binned every 500 meters. The solid circles represent the average concentration, the open triangles are the 50th percentile, and the + are the 5th and 95th percentiles for the observations within each altitude bin.

3.1: Importance of HCHO

Formaldehyde (HCHO) can be used as a proxy to estimate VOCs in the atmosphere from satellite observations because HCHO can be measured from space and is a significant intermediate in the atmospheric oxidation of VOCs. Space based observations of HCHO are not used for this analysis because they have a footprint much larger than the aircraft sampling area, typically occur during a single overpass once a day, and the retrieval on individual days can be noisy, requiring averaging over longer timeframes to produce a cleaner signal [*Harkey et al.*, 2021; *Wolfe et al.*, 2016a; *Zhu et al.*, 2016]. Due to the propensity of HCHO to stick to the walls of the sample cans and react quickly with other species, HCHO cannot be reliably stored in a whole air sampler canisters, and therefore is not measured from the can samples. Therefore, the direct measurement of HCHO, like with the NASA In-situ Airborne Formaldehyde Instrument [*Wolfe et al.*, 2016a], is the best way to quantify the ambient concentration of HCHO. For these flights, direct measurement of HCHO was not conducted, so we are not able to incorporate observations of HCHO into the analysis.

During summer months, isoprene accounts for the majority of HCHO present in the atmosphere over the NYC region [*Lin et al.*, 2012; *Luecken et al.*, 2012; *Luecken et al.*, 2018; *Lv et al.*, 2019; *Wolfe et al.*, 2016a]. This flight campaign was conducted during the meteorological spring, so rather than isoprene, anthropogenic VOCs and primary emissions of HCHO are likely the dominant sources of HCHO in the atmosphere. Other VOCs not measured in this campaign are also likely significant sources of atmospheric HCHO, like terpenes and ethylene [*Franco et*

276   *al.*, 2022; *Luecken et al.*, 2018]. Without direct measurement of these VOCs, we cannot

277   comment on their decomposition leading to HCHO production in the atmosphere.

278   A box model was used to assess the potential production of HCHO from propylene and

279   isoprene. These VOCs have similar atmospheric lifetimes (hours) and potential O_3 production,

280   but propylene has an anthropogenic and isoprene has a biogenic source. The Framework for 0-

281   Dimensional Atmospheric Modeling (F0AM) box model [*Wolfe et al.*, 2016b] uses the Master

282   Chemical Mechanism (MCM) version 3.3.1 chemical mechanism and accounts for the diurnal

283   cycle. The model is constrained to all measured atmospheric species at the time of day the can

284   was collected. Each simulation is initialized with 0 ppb of HCHO and calculates HCHO based on

285   the VOCs present and their reactions within the MCM. Three different simulations are conducted

286   for each can: 1. All VOCs are initialized with observed values (All VOC), 2. All VOCs except

287   isoprene are initialized with observed values (No Isoprene) and 3. All VOCs except propylene

288   are initialized with observed values (No Propylene). Concentrations of HCHO are reported for

289   each simulation 1 hour after model initialization. This timeframe allows important chemistry to

290   occur and produce HCHO quickly but limits concentrations from building up in the model due to

291   reactions that happen at long time scales. F0AM cannot reliably be used to estimate the

292   concentrations of HCHO that likely would have been sampled in each can because it cannot

293   account for primary emissions or the amount of HCHO already produced from VOC oxidation in

294   the atmosphere prior to sampling. As stated above, the model calculated HCHO is likely an

295   underestimation therefore, its strength resides in determining the relative contribution of

296   individual VOCs to potential HCHO production. By comparing the "No Isoprene" simulations to

297   the "All VOC" simulations, we determine the relative importance of isoprene to potential HCHO

298   production for each can. The same is done using the No Propylene simulations to estimate the

299   importance of propylene to potential HCHO production for each can. The percentage of HCHO

300   produced in the box model for each can based on isoprene and propylene concentrations are

301   calculated. The mean and median values of these percentages are 4.51% and 2.98% from

302   isoprene and 24.70% and 25.16% from propylene; the HCHO calculations for these F0AM

303   simulations can be found in supplemental information (Table S4). Based on these results, it is

304   likely that only a small fraction of the total HCHO produced from VOCs in the middle of the

305   PBL came from isoprene. For Spring 2017 in the NYC, LIS, and CT region, anthropogenic

306   VOCs play an important and possibly dominant role in HCHO formation and O_3 production.

307

308   **3.2: Reactivity with OH**

309   Reaction of VOCs with OH initiates a series of chemical reactions that form oxidants and

310   lead to photochemical O_3 production as well as secondary organic aerosols. Therefore, rate

311   constants for the reaction of VOCs with OH (k_{OH}) are the primary factor for determining

312   individual contributions of various VOCs to the formation of secondary pollutants [*Carter*, 1994;

313   *Kansal*, 2009]. VOCs can also react with O_3, however this reaction is usually slower than the

314   reaction with OH. Nevertheless, O_3 consumption rates are underestimated when solely

315   considering k_{OH}.

316   Rate constant equations for the reaction of OH with each VOC in this analysis are

317   included in Table S1. All 50 VOC species measured are ranked by their OH reactivity during this

318   sampling period, to determine which species are most important for photochemical O_3 formation.

319   In Figure 4a, the 12 VOCs with the highest median OH reactivity values for all cans are shown

320   as green bars. Median OH reactivity values for the listed VOCs are also shown for cans collected

321   in the morning (blue bars) and in the afternoon (red bars), highlighting important diurnal

322   differences. Median OH reactivity is calculated by converting the median concentration of each

323   VOC from ppbv to molecules/cm^3, accounting for pressure and temperature, and multiplying this

324   value by the rate constant k_{OH}. The median and mean observed concentrations for each VOC are

325   included in Table S1.

326   The morning reactivity of VOCs exceeds afternoon reactivity (Figure 4) due to the larger

327   abundance of VOCs earlier in the day compared to the afternoon. The morning excess may be

328   due to 1) a build-up of overnight emissions that are likely anthropogenic VOCs (note: little

329   biogenic isoprene is emitted at night) resulting in larger morning concentrations prior to peak

330   solar insolation; 2) photochemical break-down of VOCs throughout the day; or 3) morning

331   emissions of VOCs being higher than in the afternoon. Of course, all three factors could play a

332   role. Larger concentrations of VOCs in the morning likely lead to increased abundances of O_3

333   precursors during the day due to the cascade of associated chemical reactions that form HO_2 and

334   peroxy radicals upon degradation of VOCs, and lead to a rise in O_3 concentrations later in the

335   day. Figure 4b shows the median values of OFP for the 12 VOCs with the largest contribution to

336   ozone formation. The MIR values used for these calculations are included in the supplemental

337   information (Table S1). The equivalent figure showing the OH reactivity and OFP sorted by

338   mean value (rather than median) is shown in Figure S5.
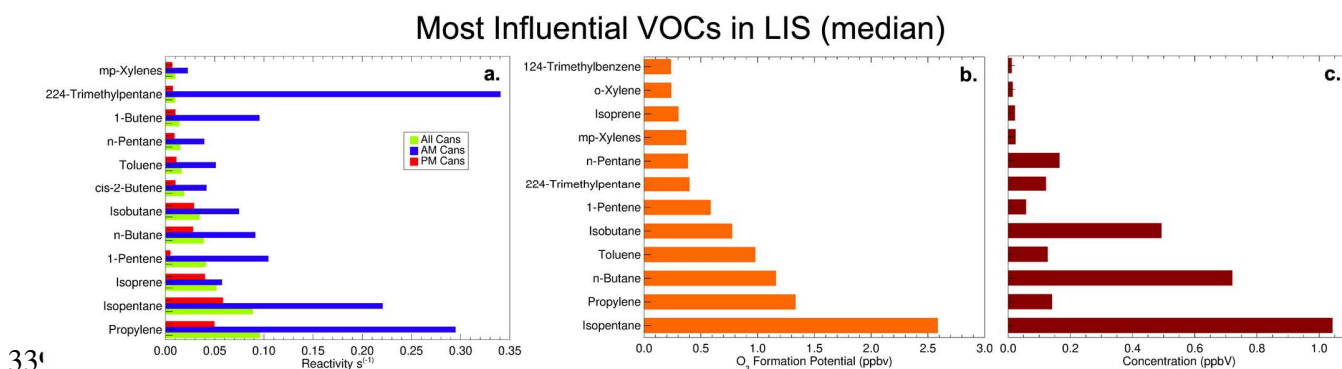
Figure 4: (a) VOCs ranked by their reactivity with OH. Values are for the median reactivity of all VOCs. The green bars represent all observations collected during the flight campaign, the blue bars represent observations collected during the morning hours, and red bars represent observations collected during the afternoon hours. (b) All VOC

343 observations are ranked by their Ozone Formation Potential (OFP) and sorted by the median OFP. (c) The
344 corresponding median VOC concentration for each VOC species is shown.

345 Isoprene is the 3rd most important VOC according to OH reactivity (Figure 4a) but 10th

346 according to OFP (Figure 4b). Isoprene has a high reactivity and MIR value indicating that under

347 the right circumstances, isoprene can contribute significantly to the production of O$_3$ (Table S1).

348 In our can samples, the concentration of isoprene is much lower than that of many other VOCs,

349 so the contribution of isoprene to O$_3$ formation is relatively small (Figure 4b) despite this large

350 reactivity. Based on these observations collected during the spring in the NYC/CT/LIS region, it

351 is likely that strong biogenic sources of isoprene such as oak trees are not yet fully leafed and

352 therefore are not emitting enough isoprene to compete with anthropogenic VOC sources. This

353 means the relative concentration of biogenic isoprene is low compared to other anthropogenic

354 VOCs.

355 As discussed above, our F0AM box-model calculations showed that only ~5% of the

356 HCHO produced in the model is directly related to isoprene concentrations, while 25-30% is due

357 to propylene. This finding means that regardless of the concentration of HCHO, the dominant

358 atmospheric source appears to be the oxidation of propylene and likely other anthropogenic

359 VOCs, rather than isoprene. Without direct measurement of HCHO, a complete understanding of

360 VOC oxidation in the atmosphere is not possible. Therefore, follow-up studies using in situ

361 aircraft observations of HCHO are necessary to provide context for the VOC observations and

362 provide a means to assess the validity of VOC representation in chemical mechanisms used in

363 models.

364 Atmospheric lifetimes of VOCs are critical components of their respective contributions

365 to local O$_3$ formation. Propylene, mainly emitted from polypropylene production, petrochemical

366 facilities and diesel exhaust [*Buzcu and Fraser*, 2006; *Hocking*, 2005; *Liu et al.*, 2008], has a

367   daytime atmospheric lifetime of $\sim$5 hours [*Atkinson*, 2000; *Warneke et al.*, 2004]. Isopentane has

368   a longer lifetime of $\sim$1 day and is emitted mainly from gasoline evaporation and engine exhaust

369   [*Buzcu and Fraser*, 2006; *Liu et al.*, 2008]. Isoprene which is biogenically produced, and HCHO

370   mainly generated from secondary reactions in the atmosphere but also produced from

371   petrochemical facilities and vehicle emissions [*Lin et al.*, 2012; *Parrish et al.*, 2012], have

372   atmospheric lifetimes of $\sim$1-2 hours [*Atkinson*, 2000; *Warneke et al.*, 2004].

373   As the day proceeds and air is convected and advected off the surface, isoprene is quickly

374   removed by reaction with OH resulting in longer-lived anthropogenic VOCs becoming more

375   important contributors to the local and transported O_3 formation. Isoprene also reacts quickly

376   with NO_3 at night, resulting in consistent lifetimes for daytime and nighttime chemistry.

377   Propylene has a longer nighttime lifetime of ~16 hours as its reaction with NO_3 is much slower

378   than that of isoprene. This allows for propylene to buildup up in the atmosphere at night while

379   isoprene is removed [*Warneke et al.*, 2004]. Therefore, as isoprene is quickly removed during all

380   times of the day, longer-lived anthropogenic VOCs can become more important contributors to

381   local and transported O_3 formation.

382

383   **3.3: Ozone Formation Potential**

384   All VOCs measured during this campaign were also classified by their chemical

385   classification category, and the resulting OFP for each category is shown in Figure 5. This

386   analysis does not include HCHO as it was not measured. The measurements of each VOC from

387   the 35 cans collected are first sorted by mixing ratio (ppbv), from highest to lowest. The average

388   of the top 10% of measurements for each VOC is found, representing an average of the largest

389   values measured during this campaign. The OFP for each VOC is then calculated using the top

390   10% average described above, and classified into one of the following categories: alkane,

391   aromatic, alkene (c3), alkene (c4), alkene (c5), alkene (c6), as shown in Figure 5a. This process

392   is repeated using the average of the middle 20% of the can measurements, and shown in Figure

393   5b. The bars in Figure 5 show the O_3 formation potential due to the various VOC categories for

394   the worst case (top 10%) and median case (middle 20%) for May 17 and 18, 2017 in the

395   NYC/LIS region. The values reported in Figure 5 are similar to Figure 12 of *Kleinman et al.*

396   [2005], who examined the reactivity associated with each VOC category for multiple

397   metropolitan regions, including NYC. For the RAMMPP observations, the flight tracks are more

398   directly downwind of NYC along LIS and more VOCs are measured than reported by *Kleinman*

399   *et al.* [2005] from the NARSTO-NE campaign conducted in 1996 [*Solomon et al.*, 2000].

400   The bar for each VOC group in Figure 5 has black lines indicating the OFPs for the

401   individual contributing species in the category (numerical values are listed in the supplementary

402   material Table S5), and the total number of contributing species to the group is shown in

403   parentheses at the end of the bar. The OFP for the alkane group is comparatively large because

404   26 alkanes were measured (over half of all VOCs measured). Isopentane is the most prominent

405   VOC is this category. Propylene is the only VOC in the alkene (c3) category and accounts for

406   significant amounts of O_3 formation potential, while isoprene is in the alkene (c5) category and

407   makes a relatively small contribution to OFP (see Table S5 for numerical values).
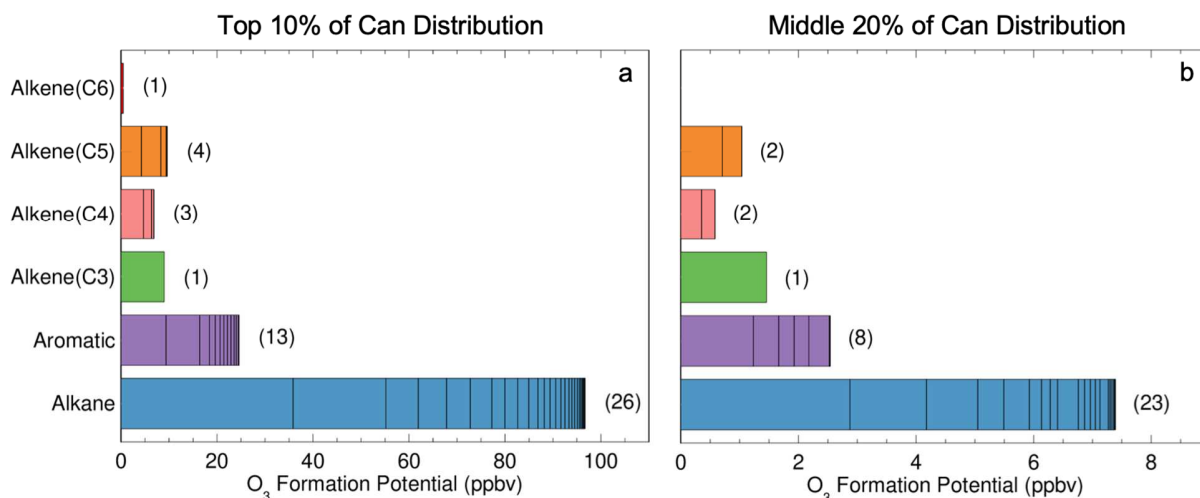
Figure 5: Ozone formation potential for the categories of hydrocarbons for the (a) top 10% of measurements and the (b) middle 20% of measurements for all VOCs measured throughout the RAMMPP 2017 flight campaign. Isoprene is the first section of the C5 bars in (a) and the second section in (b). Analysis is similar to Figure 12 from *Kleinman et al.* [2005]. OFP values for each VOC are listed in Table S5.

The results described above provide evidence that anthropogenic VOCs are playing a very important role in the photochemical production of O_3 over CT and LIS. However, given the sample size and short duration of these flights, further *in situ* observations of air both at the surface and aloft, at various times throughout the O_3 season, along with measurements of HCHO, are needed to confirm this result is representative of general conditions in the NYC metropolitan region. Continued monitoring of important species like NO_x, O_3, and VOCs in the LIS region would improve confidence in the conclusion that implementing emission controls that target the most important anthropogenically produced VOCs would improve air quality in the NYC/LIS/CT region.

4: Conclusions

Aircraft measurements of VOCs obtained during May 17 and 18, 2017 over the New York City (NYC) metropolitan area, Long Island Sound (LIS), and Connecticut (CT) suggest

426 anthropogenic VOCs contribute significantly to photochemical O_3 production. A total of 35

427 canisters were collected and 50 VOC species were quantified. Our analysis indicates the relative

428 importance of anthropogenic VOCs like isopentane and propylene (propene) to the formation of

429 O_3 is larger than that of isoprene, a mainly biogenic VOC. This finding may be due to the short

430 lifetime of isoprene (~1-2 hours) compared to many anthropogenic VOCs and/or minimal

431 isoprene emissions in the NYC metro region at this time of year, resulting in the greater relative

432 impact of longer-lived anthropogenic VOCs to O_3 formation.

433   Since formaldehyde (HCHO) was not measured during these flights, we use a 0-D box

434 model to estimate the percentage of HCHO produced by propylene and isoprene based on their

435 observed concentrations. Only ~5% of the HCHO produced in the model is due to the breakdown

436 of isoprene, while 25-30% is due to propylene degradation. This result shows that the likely

437 sources of HCHO in the atmosphere for this flight campaign are predominantly anthropogenic in

438 nature, and not from isoprene.

439   Air circulating aloft within the Planetary Boundary Layer (PBL) cannot quickly replenish

440 with VOCs and other pollutants emitted from the surface. This isolation can create an O_3

441 photochemical production regime that differs from the surface, complicating our understanding

442 of O_3 production within the PBL. Conditions like this may exist over bodies of water and during

443 early spring and late fall months when biogenic VOC sources are significantly reduced.

444 Therefore, the longer-lived anthropogenic VOCs and other anthropogenic pollutants remain in

445 these air parcels and are carried downwind contributing to poor air quality in relatively distant

446 regions, particularly when transported over bodies of water such as LIS.

447   The data collected during this measurement campaign also provide evidence for the

448 diurnal variation of the concentration of mid-PBL VOCs. When the VOCs are sorted by time of

449   day, morning VOC reactivity (blue bars in Figure 4a) is much greater than afternoon reactivity

450   (red bars in Figure 4a). This finding indicates that in the NYC metropolitan region and areas

451   downwind, VOCs emitted overnight and in early morning hours when photochemistry is inactive

452   and isoprene is scavenged by NO_3 [*Warneke et al.*, 2004] may contribute to a build-up of

453   anthropogenic VOCs near the surface. As the sun rises and photochemistry resumes, the high

454   morning concentrations of VOCs will form HO_2 and peroxy radicals, which contribute to high

455   afternoon concentrations of O_3. As atmospheric conditions evolve from VOC-sensitive in the

456   morning hours to NO_x-sensitive in the afternoon [*Chen and Brune*, 2012; *Mao et al.*, 2010], the

457   atmosphere likely transitions through conditions where the MIR and OFP values discussed in

458   this work are applicable, producing the maximum amount of O_3. Therefore, controlling the

459   emission of anthropogenic VOCs, especially in the early morning and overnight hours, may help

460   reduce the maximum concentrations of O_3 that are usually reached in the afternoon.

461   Previous studies indicate near-surface air over large bodies of water like LIS or Lake

462   Michigan (downwind from Chicago) is likely VOC-sensitive due to stagnant meteorology,

463   heavily polluted air, and suppressed PBL heights [*Sillman et al.*, 1993]. Therefore, surface

464   measurements of VOCs and NO_x may not fully explain photochemical O_3 production for

465   conditions aloft (250 to ~1500 m) [*Kleinman*, 2000; *Sillman*, 1999] in air parcels depleted in

466   isoprene over these bodies of water. The O_3 production from anthropogenic VOCs could have

467   important implications for air quality attainment strategies for municipalities downwind of

468   metropolitan areas such as NYC, where the vertical mixing of the boundary layer can bring

469   VOCs and any O_3 produced in the pollution plume down to the surface [*Sillman*, 1999; 2002;

470   *Sillman et al.*, 1993]. Importantly, surface monitoring may not measure the VOCs most critical to

471   air quality aloft. As industry develops, new technologies are implemented, and societal activity

472 changes, the atmospheric composition of anthropogenic VOCs will likely evolve. Therefore,

473 continued monitoring of VOCs at the surface and aloft is critical to understanding the

474 complicated photochemistry that leads to O_3 production in areas designated as in non-attainment

475 of the NAAQS O_3 standard like the NYC region.

476   While many important VOCs were measured during LISTOS, the observations not

477 exhaustive. The data from the May 17 and 18 2017 flights did not include ethylene, another

478 important and abundant VOC with both anthropogenic and biogenic sources that contributes

479 significantly to HCHO formation [*Franco et al.*, 2022]. Ethylene is measured at surface PAMS

480 monitors, however the first concentrations reported in 2017 are for May 31, almost two weeks

481 after the data discussed in this paper was collected. Flights conducted as part of the LISTOS field

482 mission in 2019 report measurements of ethylene and HCHO but analysis of these cans is

483 beyond the scope of this paper. As is evidenced by *McDonald et al.* [2018] and *Coggon et al.*

484 [2021], future field missions should expand measurement capabilities beyond the well-monitored

485 primary VOCs to also included Volatile Chemical Products (VCPs) and terpenes. These missing

486 classes of VOCs have been shown to impact O_3 production in urban regions, specifically the

487 New York metropolitan region and are critical to improving modeling capabilities in these

488 regions. Gathering direct measurements of these species will provide comparison opportunities

489 for large air quality models when emission inventories are further speciated to account for these

490 VOCs. Moving forward, the air quality community must continue using a multifaceted approach,

491 including satellite observations such as those to be provided by the upcoming Tropospheric

492 Emissions: Monitoring of Pollution (TEMPO) mission [*Zoogman et al.*, 2017], surface

493 monitoring, and aircraft measurements of various VOCs and VCPs to understand the

494 complexities of atmospheric O_3 formation.

References

516   **References**

517   AirNow (Accessed 2018), AirNow, edited, p. https://www.airnow.gov/.
518

519   Atkinson, R. (2000), Atmospheric chemistry of VOCs and NOx, *Atmospheric Environment*, *34*(12-14), 2063-2101,
520   doi:Doi 10.1016/S1352-2310(99)00460-4.
521

522   Baker, A. K., A. J. Beyersdorf, L. A. Doezema, A. Katzenstein, S. Meinardi, I. J. Simpson, D. R. Blake, and F.
523   Sherwood Rowland (2008), Measurements of nonmethane hydrocarbons in 28 United States cities,
524   *Atmospheric Environment*, *42*(1), 170-182, doi:10.1016/j.atmosenv.2007.09.007.
525

526   Buzcu, B., and P. Fraser (2006), Source Identification and Apportionment of Volatile Organic Compounds in
527   Houston, TX, *Atmospheric Environment*, *40*, 2385-2400.
528

529   Caicedo, V., R. Delgado, W. T. Luke, X. Ren, P. Kelley, P. R. Stratton, R. R. Dickerson, T. A. Berkoff, and G.
530   Gronoff (2021), Observations of bay-breeze and ozone events over a marine site during the OWLETS-2
531   campaign, *Atmospheric Environment*, *263*, doi:10.1016/j.atmosenv.2021.118669.
532

533   Carter, W. P. L. (1994), Development of Ozone Reactivity Scales for Volatile Organic Compounds, *Journal of Air*
534   *& Waste Management Association*, *44*(7), 881-899, doi:10.1080/1073161X.1994.10467290.
535

536   Carter, W. P. L. (2010), Updated Maximum Incremental Reactivity Scale and Hydrocarbon Bin Reactivities for
537   Regulatory Applications, *California Air Resources Board Contract 07-339*,
538   https://www.arb.ca.gov/regact/2009/mir2009/mir2010.pdf.
539

540   Chen, S., and W. H. Brune (2012), Global sensitivity analysis of ozone production and O3–NOx–VOC limitation
541   based on field data, *Atmospheric Environment*, *55*, 288-296, doi:10.1016/j.atmosenv.2012.03.061.
542

543   Chen, X., et al. (2019), On the sources and sinks of atmospheric VOCs: an integrated analysis of recent aircraft
544   campaigns over North America, *Atmospheric Chemistry and Physics*, *19*(14), 9097-9123, doi:10.5194/acp-
545   19-9097-2019.
546

547   Coggon, M. M., et al. (2021), Volatile chemical product emissions enhance ozone and modulate urban chemistry,
548   *Proc Natl Acad Sci U S A*, *118*(32), doi:10.1073/pnas.2026653118.
549

550   EPA (1970), The Clean Air Act, edited, Title 42, Chapter 85 United States Congress §7401 et seq.,
551   https://www.epa.gov/laws-regulations/summary-clean-air-act.
552

553   EPA (1990), Clean Air Act Amendments of 1990, in *Public Law*, edited.
554

555   EPA (2016a), NAAQS Table, *Criteria Air Pollutants*, https://www.epa.gov/criteria-air-pollutants/naaqs-table.
556

557   EPA (2016b), Technical Assistance Document for the National Air Toxics Trends Stations Program, *Revision 3*,
558   https://www3.epa.gov/ttnamti1/files/ambient/airtox/NATTS%20TAD%20Revision%203_FINAL%220Oct
559   ober%202016.pdf.
560

561   Federal_Register (2022a), Determinations of Attainment by the Attainment Date, Extensions of the Attainment
562   Date, and Reclassification of Areas Classified as Marginal for the 2015 Ozone National Ambient Air
563   Quality Standards, *Federal Register*, *87*(68097).
564

565   Federal_Register (2022b), Determinations of Attainment by the Attainment Date, Extensions of the Attainment
566   Date, and Reclassification of Areas Classified as Serious for the 2008 Ozone National Ambient Air Quality
567   Standards, *Federal Register*, *87*(60926).
568

569   Franco, B., L. Clarisse, M. Van Damme, J. Hadji-Lazaro, C. Clerbaux, and P. F. Coheur (2022), Ethylene industrial
570   emitters seen from space, *Nat Commun*, *13*(1), 6452, doi:10.1038/s41467-022-34098-8.

571
572 Han, Z. S., J. E. González-Cruz, H. N. Liu, D. Melecio-Vázquez, H. Gamarro, Y. H. Wu, F. Moshary, and R.
573   Bornstein (2022), Observed sea breeze life cycle in and around NYC: Impacts on UHI and ozone patterns,
574   *Urban Climate*, *42*, doi:10.1016/j.uclim.2022.101109.
575
576 Harkey, M., T. Holloway, E. J. Kim, K. R. Baker, and B. Henderson (2021), Satellite Formaldehyde to Support
577   Model Evaluation, *J Geophys Res Atmos*, *126*(4), doi:10.1029/2020jd032881.
578
579 He, H., et al. (2013), Trends in emissions and concentrations of air pollutants in the lower troposphere in the
580   Baltimore/Washington airshed from 1997 to 2011, *Atmospheric Chemistry and Physics*, *13*(15), 7859-7874,
581   doi:10.5194/acp-13-7859-2013.
582
583 Hembeck, L., H. He, T. P. Vinciguerra, T. P. Canty, R. R. Dickerson, R. J. Salawitch, and C. Loughner (2019),
584   Measured and modelled ozone photochemical production in the Baltimore-Washington airshed,
585   *Atmospheric Environment: X*, *2*, doi:10.1016/j.aeaoa.2019.100017.
586
587 Hocking, M. B. (2005), *Handbook of Chemical Technology and Pollution Control*, 830 pp., Academic Press,
588   doi:10.1016/B978-0-12-088796-5.X5000-5.
589
590 Kansal, A. (2009), Sources and Reactivity of NMHCs and VOCs in the Atmopshere: A Review, *Journal of
591   Hazardous Materials*, *166*, 17-26, doi:10.1016/j.jhazmat.2008.11.048.
592
593 Kleinman, L. I. (2000), Ozone process insights from field experiments - part II: Observation-based analysis for
594   ozone production, *Atmospheric Environment*, *34*(12-14), 2023-2033, doi:Doi 10.1016/S1352-
595   2310(99)00457-4.
596
597 Kleinman, L. I., P. H. Daum, Y. N. Lee, L. J. Nunnermacker, S. R. Springston, J. Weinstein-Lloyd, and J. Rudolph
598   (2005), A comparative study of ozone production in five U.S. metropolitan areas, *110*(D2),
599   doi:10.1029/2004jd005096.
600
601 Li, H., et al. (2020), Terpenes and their oxidation products in the French Landes forest: insights from Vocus PTR-
602   TOF measurements, *Atmospheric Chemistry and Physics*, *20*(4), 1941-1959, doi:10.5194/acp-20-1941-
603   2020.
604
605 Lin, Y. C., J. J. Schwab, K. L. Demerjian, M.-S. Bae, W.-N. Chen, Y. Sun, Q. Zhang, H.-M. Hung, and J. Perry
606   (2012), Summertime formaldehyde observations in New York City: Ambient levels, sources and its
607   contribution to HOx radicals, *Journal of Geophysical Research: Atmospheres*, *117*(D8), n/a-n/a,
608   doi:10.1029/2011jd016504.
609
610 Liu, Y., M. Shao, L. Fu, S. Lu, L. Zeng, and D. Tang (2008), Source Profiles of Volatile Organic Comounds (VOCs)
611   Measured in China: Part 1, *Atmospheric Environment*, *42*, 6247-6260.
612
613 Loughner, C. P., et al. (2014), Impact of Bay-Breeze Circulations on Surface Air Quality and Boundary Layer
614   Export, *Journal of Applied Meteorology and Climatology*, *53*(7), 1697-1713, doi:10.1175/Jamc-D-13-
615   0323.1.
616
617 Luecken, D. J., W. T. Hutzell, M. L. Strum, and G. A. Pouliot (2012), Regional sources of atmospheric
618   formaldehyde and acetaldehyde, and implications for atmospheric modeling, *Atmospheric Environment*, *47*,
619   477-490, doi:10.1016/j.atmosenv.2011.10.005.
620
621 Luecken, D. J., S. L. Napelenok, M. Strum, R. Scheffe, and S. Phillips (2018), Sensitivity of Ambient Atmospheric
622   Formaldehyde and Ozone to Precursor Species and Source Types Across the United States, *Environ Sci
623   Technol*, *52*(8), 4668-4675, doi:10.1021/acs.est.7b05509.
624

Lv, S.-Y., Q.-Y. Liu, Y.-X. Zhao, M.-Q. Zhang, L.-X. Jiang, and S.-G. He (2019), Formaldehyde Generation in Photooxidation of Isoprene on Iron Oxide Nanoclusters, *The Journal of Physical Chemistry C*, *123*(8), 5120-5127, doi:10.1021/acs.jpcc.8b12471.

MaineDEP (2017), Standard Operating Procedure for the Determination of Volatile Organic Compounds (VOCs) in Air Collected in Specially-Prepared Canisters and Analyzed by Gas Chromatography/Mass Spectrometry (GC/MS), *(available upon request)*, 52.

Mao, J., et al. (2010), Atmospheric oxidation capacity in the summer of Houston 2006: Comparison with summer measurements in other metropolitan studies, *Atmospheric Environment*, *44*(33), 4107-4115, doi:10.1016/j.atmosenv.2009.01.013.

Mazzuca, G. M., K. E. Pickering, R. D. Clark, C. P. Loughner, A. Fried, D. C. S. Zweers, A. J. Weinheimer, and R. R. Dickerson (2017), Use of tethersonde and aircraft profiles to study the impact of mesoscale and microscale meteorology on air quality, *Atmospheric Environment*, *149*, 55-69, doi:10.1016/j.atmosenv.2016.10.025.

McDonald, B. C., et al. (2018), Volatile chemical products emerging as largest petrochemical source of urban organic emissions, *Science*, *359*(6377), 760-764, doi:10.1126/science.aaq0524.

Parrish, D. D., et al. (2012), Primary and secondary sources of formaldehyde in urban atmospheres: Houston Texas region, *Atmospheric Chemistry and Physics*, *12*(7), 3273-3288, doi:10.5194/acp-12-3273-2012.

Ren, X., et al. (2018), Methane Emissions From the Baltimore-Washington Area Based on Airborne Observations: Comparison to Emissions Inventories, *Journal of Geophysical Research: Atmospheres*, *123*(16), 8869-8882, doi:doi:10.1029/2018JD028851.

Schwantes, R. H., et al. (2020), Comprehensive isoprene and terpene gas-phase chemistry improves simulated surface ozone in the southeastern US, *Atmospheric Chemistry and Physics*, *20*(6), 3739-3776, doi:10.5194/acp-20-3739-2020.

Seltzer, K. M., E. Pennington, V. Rao, B. N. Murphy, M. Strum, K. K. Isaacs, and H. O. T. Pye (2021), Reactive organic carbon emissions from volatile chemical products, *Atmos Chem Phys*, *21*(6), 5079-5100, doi:10.5194/acp-21-5079-2021.

Sillman, S. (1999), The relation between ozone, NOx and hydrocarbons in urban and polluted rural environments, *Atmospheric Environment*, *33*(12), 1821-1845, doi:Doi 10.1016/S1352-2310(98)00345-8.

Sillman, S. (2002), Some theoretical results concerning O3-NOx-VOC chemistry and NOx-VOC indicators, *Journal of Geophysical Research*, *107*(D22), doi:10.1029/2001jd001123.

Sillman, S., P. J. Samson, and J. M. Masters (1993), Ozone production in urban plumes transported over water: Photochemical model and case studies in the northeastern and midwestern United States, *Journal of Geophysical Research*, *98*(D7), doi:10.1029/93jd00159.

Solomon, P., E. Cowling, G. Hidy, and C. Furiness (2000), Comparison of scientific findings from major ozone field studies in North America and Europe, *Atmospheric Environment*, *34*(12-14), 1885-1920, doi:10.1016/s1352-2310(99)00453-7.

Stauffer, R. M., A. M. Thompson, D. K. Martins, R. D. Clark, D. L. Goldberg, C. P. Loughner, R. Delgado, R. R. Dickerson, J. W. Stehr, and M. A. Tzortziou (2015), Bay breeze influence on surface ozone at Edgewood, MD during July 2011, *J Atmos Chem*, *72*(3-4), 335-353, doi:10.1007/s10874-012-9241-6.

Stein, A. F., R. R. Draxler, G. D. Rolph, B. J. B. Stunder, M. D. Cohen, and F. Ngan (2015), NOAA's HYSPLIT Atmospheric Transport and Dispersion Modeling System, *Bulletin of the American Meteorological Society*, *96*(12), 2059-2077, doi:10.1175/bams-d-14-00110.1.

Tang, J. H., L. Y. Chan, C. Y. Chan, Y. S. Li, C. C. Chang, S. C. Liu, D. Wu, and Y. D. Li (2007), Characteristics and diurnal variations of NMHCs at urban, suburban, and rural sites in the Pearl River Delta and a remote site in South China, *Atmospheric Environment*, *41*(38), 8620-8632, doi:10.1016/j.atmosenv.2007.07.029.

Taubman, B. F., L. T. Marufu, C. A. Piety, B. G. Doddridge, J. W. Stehr, and R. R. Dickerson (2004), Airborn Characterization of the Chemical, Optical, and Meteorological Properties and Origins of a Combined Ozone-Haze Episode over the Eastern United States, *Journal of Atmospheric Sciences*, *61*, 1781-1793.

Torres-Vazquez, A., J. Pleim, R. Gilliam, and G. Pouliot (2022), Performance Evaluation of the Meteorology and Air Quality Conditions From Multiscale WRF-CMAQ Simulations for the Long Island Sound Tropospheric Ozone Study (LISTOS), *Journal of Geophysical Research: Atmospheres*, *127*(5), doi:10.1029/2021jd035890.

Venecek, M. A., W. P. L. Carter, and M. J. Kleeman (2018), Updating the SAPRC Maximum Incremental Reactivity (MIR) scale for the United States from 1988 to 2010, *J Air Waste Manag Assoc*, *68*(12), 1301-1316, doi:10.1080/10962247.2018.1498410.

Warneke, C., et al. (2004), Comparison of daytime and nighttime oxidation of biogenic and anthropogenic VOCs along the New England coast in summer during New England Air Quality Study 2002, *Journal of Geophysical Research*, *109*(D10), doi:10.1029/2003jd004424.

Wolfe, G. M., et al. (2016a), Formaldehyde production from isoprene oxidation across NOx regimes, *Atmos Chem Phys*, *16*(4), 2597-2610, doi:10.5194/acp-16-2597-2016.

Wolfe, G. M., M. R. Marvin, S. J. Roberts, K. R. Travis, and J. Liao (2016b), The Framework for 0-D Atmospheric Modeling (F0AM) v3.1, *Geoscientific Model Development*, *9*(9), 3309-3319, doi:10.5194/gmd-9-3309-2016.

Wu, Y., et al. (2021), Synergistic aircraft and ground observations of transported wildfire smoke and its impact on air quality in New York City during the summer 2018 LISTOS campaign, *Sci Total Environ*, *773*, 145030, doi:10.1016/j.scitotenv.2021.145030.

Zhu, L., et al. (2016), Observing atmospheric formaldehyde (HCHO) from space: validation and intercomparison of six retrievals from four satellites (OMI, GOME2A, GOME2B, OMPS) with SEAC(4)RS aircraft observations over the Southeast US, *Atmos Chem Phys*, *16*(21), 13477-13490, doi:10.5194/acp-16-13477-2016.

Zoogman, P., et al. (2017), Tropospheric Emissions: Monitoring of Pollution (TEMPO), *J Quant Spectrosc Radiat Transf*, *186*, 17-39, doi:10.1016/j.jqsrt.2016.05.008.